Article citation info:
Guemmour MB, Negadi K, Araria R, Bey M. Analysis and fault diagnosis in point absorber wave energy conversion systems using fault tree and bayesian networks. Diagnostyka. 2025;26(2):2025209. https://doi.org/10.29354/diag/204573.

DIAGNOSTYKA, 2025, Vol. 26, No. 2

e-ISSN 2449-5220
DOI: 10.29354/diag/204573

ANALYSIS AND FAULT DIAGNOSIS IN POINT ABSORBER WAVE ENERGY CONVERSION SYSTEMS USING FAULT TREE AND BAYESIAN NETWORKS

Mohamed Boutkhil GUEMMOUR [1], Karim NEGADI [2], Rabah ARARIA [2], Mohamed BEY [2]

[1] Industrial Technologies Research Laboratory, Department of Mechanical Engineering, of Applied Science, University of Tiaret, Algeria
[2] L2GEGI Laboratory, Department of Electrical Engineering, Faculty of Applied Science, University of Tiaret, Algeria
[*] Corresponding author, e-mail: karim.negadi@univ-tiaret.dz

Abstract

This paper presents a comprehensive analysis and fault diagnosis approach for wave energy conversion (WEC) systems, specifically focusing on point absorber technology, using Bayesian Networks (BNs). The main objective of this work is to develop a probabilistic framework that enhances fault detection and diagnosis by modeling the interdependencies between key subsystems, including the power take-off (PTO) mechanism, mooring lines, and electrical components. Wave energy conversion systems offer a promising solution for sustainable energy generation, but fault detection remains a critical challenge in ensuring continuous and efficient operation. The proposed approach enables a probabilistic evaluation of failure modes and their impact on overall system performance by modeling the complex interdependencies between system components. By integrating environmental factors, historical failure logs, and operational data, the Bayesian network allows real-time dynamic updates of fault probabilities, facilitating predictive maintenance techniques. The proposed approach aims to improve system reliability, reduce downtime, and optimize maintenance strategies. Case studies are provided to validate the approach, demonstrating significant improvements in early fault detection. The results underscore the potential of Bayesian networks as a powerful tool for enhancing the operational resilience and sustainability of wave energy conversion systems. The analysis focuses on key subsystems, including the power take-off mechanism, mooring lines, and electrical components, where failures are most likely to occur due to harsh marine conditions.

Keywords: wave energy converters, bayesian networks, point absorber, fault tree analysis, probabilistic modeling

List of Symbols/Acronyms

BEM Boundary Element Method;
BN Bayesian Networks;
FMEA Failure Mode, Effects, and Criticality Analysis;
FTA Fault Tree Analysis;
LPMSG Linear Permanent Magnet Synchronous Generator;
MPPT Maximum Power Point Tracking;
MSD Mass-Spring-Damper;
PA Point Absorber;
PTO Power Take-Off;
RCA Root Cause Analysis;
WEC Wave Energy Converter;
F_b – Buoyant force [N];
F_{exc} – Excitation force [N];
F_{rad} – Radiation force [N];
F_{hs} – Hydrostatic restoring force [N];
F_{PTO} – Damping Force [N];
x – Horizontal position [m];
z – Buoy motion in heave [m];
g – Gravity acceleration [m.s^{-2}];
$\dot{z}$ – Buoy velocity in heave [m.s^{-1}];
ρ – Water density [kg.m^{-3}];
M – Mass of the buoy [kg];
η – Wave surface elevation [m^2];
λ – Wavelength [m];
B_{PTO} – PTO damping coefficient [Ns/m];
B_{PTO1} – Linear damping coefficients [Ns/m];
B_{PTO2}– Non-linear damping coefficients [N.s.m^{-1}];
B – Total damping [Ns/m];
A_∞– added mass at infinite frequency [kg];
C – Hydrostatic stiffness [N/m];
h – Impulse response function of the buoy [s.m^{-1}];

1. INTRODUCTION

Wave energy conversion (WEC) systems are a promising solution for sustainable energy generation, offering a clean and continuous source of electricity. However, one of the main challenges limiting the widespread deployment of WEC technologies is ensuring their long-term reliability and operational stability in harsh marine environments. The growing demand for renewable

Received 2024-10-19; Accepted 2025-05-01; Available online 2025-05-06

energy sources has spurred significant research and development in WEC systems [1]. Frequent and unpredictable stresses from wave forces, corrosion, and biofouling can cause unanticipated failures and expensive downtime in WEC system components like power take-off (PTO) mechanisms, mooring lines, and electrical systems. The ability to predict, detect, and isolate potential faults before they lead to catastrophic failures is crucial for improving system performance and lowering maintenance costs.

Test sites such as the European Marine Energy Centre (EMEC) in Scotland and the Wave Hub facility in the UK have played a fundamental role in identifying the practical challenges associated with WEC technologies [2, 3]. These platforms have hosted various point absorber devices, including the Wello Penguin and the OE Buoy, which have experienced common operational issues like mooring system failures, generator malfunctions, and structural wear caused by harsh marine environments. Utilizing data from these real-world installations can enhance fault diagnosis methods by supporting the validation and optimization of predictive maintenance models, such as the Bayesian Network approach proposed in this work. Drawing from these practical experiences, our methodology seeks to enhance the reliability and performance of wave energy systems under actual ocean conditions.

Traditional diagnostic approaches often fall short in complex, uncertain environments like the ocean, where multiple factors interact dynamically [4]. Therefore, advanced tools that can model these uncertainties and interdependencies are needed to enhance reliability and fault management in WEC systems [5]. Good fault diagnosis and reliability analysis are essential to maintaining the operational health of WEC systems [6, 7].

In this context, Bayesian Networks (BNs) offer a powerful probabilistic framework for addressing the challenges of reliability analysis and fault diagnosis in WEC systems. Bayesian networks can model the relationships between system components, incorporate both expert knowledge and real-time data, and dynamically update fault probabilities as new information becomes available [8]. This allows for more accurate predictions of failure modes and quicker identification of faults, enabling proactive maintenance strategies and minimizing downtime.

This research suggests a thorough method for defect diagnosis and reliability analysis in WEC systems using Bayesian networks [9]. Through the integration of environmental parameters, component failure histories, and operational data, the model offers a strong analytical tool for examining the intricate interdependencies seen in WEC systems. Through case studies including critical subsystems where failures are most common, such as the PTO and mooring lines, we illustrate the efficacy of this approach [10]. The findings demonstrate that Bayesian networks are a crucial tool for wave energy technology in the future since they greatly improve fault identification early on and increase overall system reliability [11, 12].

This study aims to address this challenge by developing a fault diagnosis approach based on Bayesian Networks, capable of capturing the strong coupling between electrical, mechanical, and control subsystems.

The paper is organized as follows: first, after an introduction, the synopsis of the case study is given in second section. Second, the modelling of maritime conversion utilizing a point absorber approach is described in section 3. The electrical analysis of a wave energy-based pint absorber is provided in Section 3. Section 4 focuses on the practical application of WEC station based Bayesian networks for diagnosis study. The analysis, results of simulation and discussion are shown in Section 5. Section 6 concludes by summarizing the research's primary conclusions and outlining possible directions for future research.

2. POINT ABSORBER TECHNOLOGY

Point Absorber technology, designed for harnessing wave energy, faces several potential faults that can significantly impact its performance and reliability. These faults arise across its mechanical, electrical, and control systems due to the harsh marine environment and complex interdependencies between components [13]. Figure 1 illustrates the components of a marine conversion chain based on the point absorber, as well as the various types of faults that can occur in this type of industrial installation.

Mechanical faults are common in the buoy and mooring systems. The buoy is subject to continuous wave impacts, leading to structural fatigue and possible material failure, which reduces its ability to absorb energy effectively [14]. Corrosion is another critical issue, as prolonged exposure to seawater can degrade mechanical components, especially mooring lines, causing them to break or weaken. A broken mooring line can cause the buoy to drift, severely affecting energy capture [15].

In the power take-off system, faults such as wear and tear in moving parts like bearings and gears reduce energy conversion efficiency [16]. Hydraulic PTO systems may suffer from fluid leaks, resulting in power losses and reduced system output. Increased frictional losses in mechanical PTO systems also degrade performance over time.

Electrical faults in the generator, particularly in the Linear Permanent Magnet Synchronous Generator (LPMSG), can include short circuits due to insulation breakdown, voltage instability caused by faulty inverters, and overheating from excessive operational loads or cooling system failures [17]. These faults can disrupt energy production and potentially damage components.

Control system faults may arise from failures in the Maximum Power Point Tracking (MPPT) algorithms or real-time monitoring systems, leading

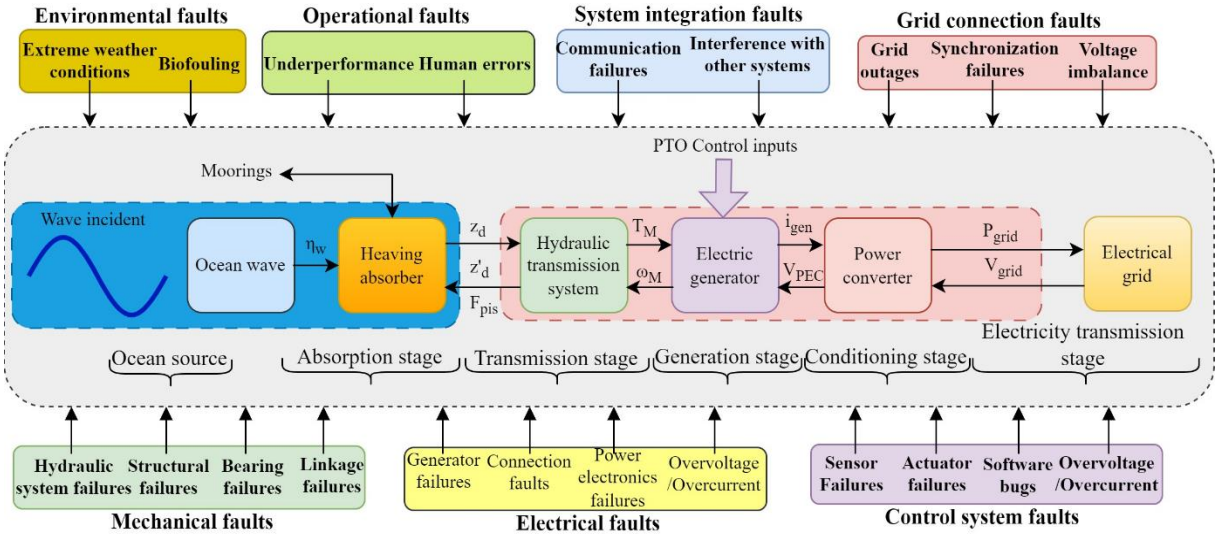

Fig. 1. Categorization of failure modes and analysis of subsystem interdependencies in point absorber wave energy conversion systems

to suboptimal energy capture. Grid synchronization issues can also occur during fluctuations in wave power, causing energy losses or temporary disconnections from the grid [18].

Finally, environmental factors like extreme weather events, such as storms or rogue waves, can impose excessive stress on the system, damaging mechanical and electrical components [19]. Additionally, marine growth on the buoy and mooring lines can increase drag, reducing the buoy's motion and overall energy efficiency.

Mitigating these faults requires robust maintenance strategies, real-time fault detection systems, and adaptive control mechanisms to ensure the longevity and efficiency of Point Absorber systems in challenging marine environments.

One kind of wave energy converter that uses energy from ocean waves is a point absorber [20]. Figure 2 shows a well-known example of a body point absorber (PA) with self-reacting capabilities. The OPT power buoy device [21] exemplifies a design widely utilized in wave energy conversion due to its efficiency and adaptability. A point absorber is modeled from both an electrical and hydrodynamic perspective. Figure 3 provides a representative illustration of a self-reacting point absorber, demonstrating how the device effectively captures ocean wave energy for power generation.

To illustrate the idea and layout of a wave energy converter, a simple sketch might be utilized. The primary purpose of a WEC is to convert the kinetic and potential energy of waves in the ocean into electrical power that can be used [22]. In the sketch, you might illustrate how a buoyant building rises and falls in response to the passing waves. This buoy is attached to a mechanical linkage that, as shown in Fig. 3, transforms the vertical motion into mechanical motion. This linkage is often in the form of a piston or hydraulic system. This mechanical energy is received by the generator, which is visualized as a box with coils and magnets, and it is used to produce electricity [23]. The generator is connected to an electrical output that can be sent into the electricity grid or used to charge a local energy storage device that runs on batteries. The drawing may also incorporate sensors and control devices to optimize energy capture and adapt to shifting wave conditions. The basic concept is that wave motion can be transformed into mechanical motion and then into electrical energy by a well-designed WEC system.

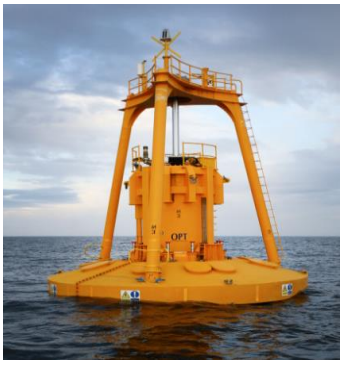

Fig. 2. One popular example of a body PAs that may self-react is the OPT power buoy device [25].

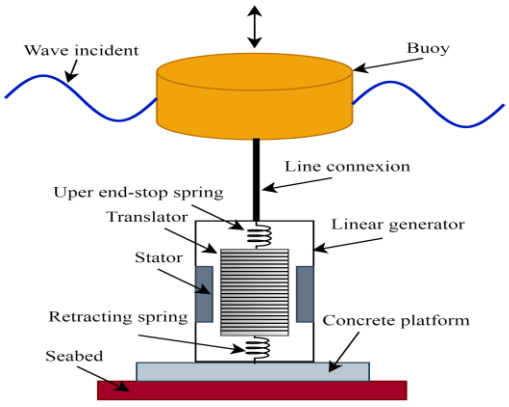

Fig. 3. Concept and layout of the WEC in a sketch [23]

Figure 4 depicts the simplified electrical schematic of a point absorber for maritime energy conversion, which encapsulates the fundamental elements and actions of the system.

It usually comprises of a power take-off component that acts as a voltage source with an internal impedance to convert the buoyant structure's mechanical motion into electrical power [24]. Batteries and capacitors, two common energy storage components, are used to store and control the generated energy.

Depending on the needed output, the circuit may comprise rectifiers and inverters. Control systems are necessary to ensure smooth operation and boost the efficiency of power capture. Ultimately, the items that consume the generated electricity are represented by the electrical load.

3. DETAILED MODELING OF POINT ABSORBER WAVE ENERGY CONVERTER FOR DIAGNOSTIC STUDY

A detailed modeling of the point absorber's physical interaction with ocean waves, the dynamics of the power take-off system, and failure mechanisms are all part of the detailed modeling that is necessary to develop a comprehensive model of a point absorber wave energy converter for reliability and diagnostic studies. Three main areas of focus are hydrodynamic modeling, mechanical and electrical reliability, and diagnostic methodologies.

3.1. Wave theory

The propagation of small amplitude waves on the surface of a fluid is described by the fundamental wave equation, which is derived from linear wave theory as shown in Fig. 5. The two-dimensional equation, which takes time t and horizontal displacement along the x-axis into account, is as follows [26]:

$$\frac{\partial^2 \eta}{\partial t^2} = c^2 \frac{\partial^2 \eta}{\partial x^2} \tag{1}$$

where:
$\eta(x,t)$: represents the wave surface elevation as a function of position x and time t.
c: is the phase speed of the wave, which depends on the properties of the fluid and the wave.
The phase speed for deep water waves can be expressed as:

$$c = \sqrt{\frac{g}{k}} \tag{2}$$

where:
g : is the acceleration due to gravity.
k : is the wave number, given by $k = \frac{2\pi}{\lambda}$
λ : is the wavelength.

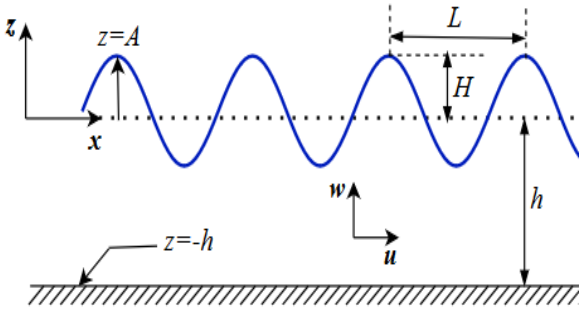

Fig. 5. Wave shape with sinusoidal incidence

$$\eta(x,t) = \frac{A\omega}{k} sin(kx - \omega t) \tag{3}$$

where:
η: is the elevation of the free surface with respect to z = 0 (m)
A: corresponds to the wave's amplitude (m).
k: is the wave number (rad/m).
ω: is the angular motion frequency (rad/s).
x: is the position horizontally (m).
t: is the time (s).

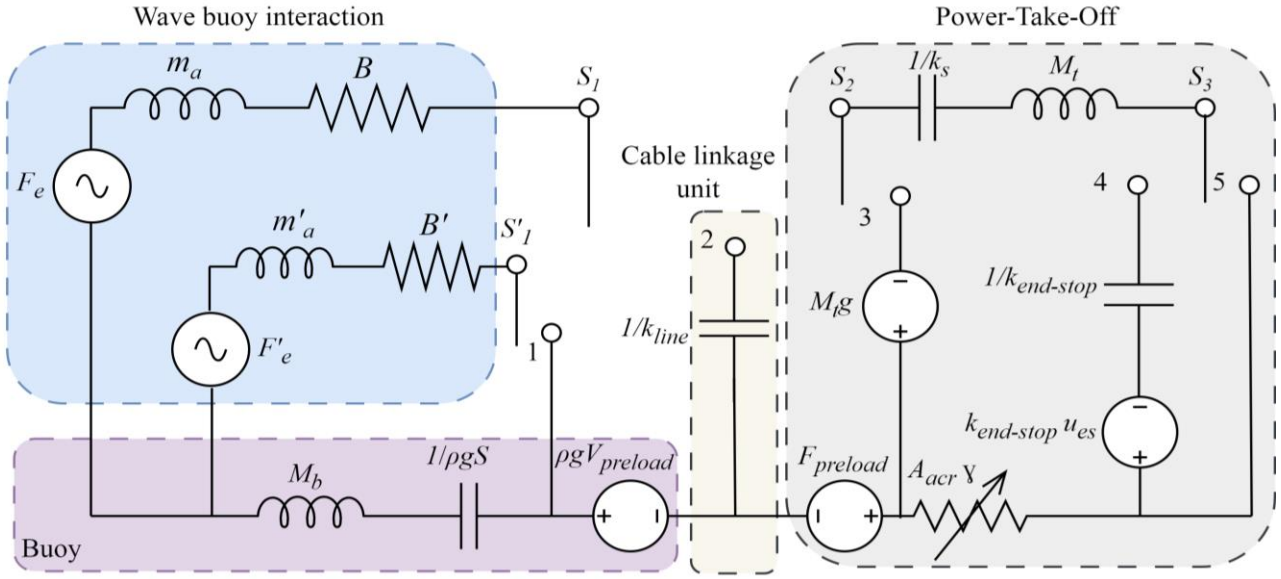

Fig. 4. Marine energy point absorber equivalent circuit diagram

Estimating the kinetic energy of the incident waves requires knowledge of this velocity.

The Archimedes principle [27] can be used to compute the buoyancy force operating on the point absorber.

$$F_b = \rho_\omega g V \tag{4}$$

where:
F_b: is the buoyant force (N).
ρ_ω: is the density of the water (kg/m^3).
g: is gravity's cause of acceleration (m/s^2).
V: is the volume that has been moved by the point absorber (m^3).

Equation [5] can be used to determine the electrical power that the point absorber has absorbed.

$$P_e = \frac{1}{2}\rho_\omega g V H_s C_d v^3 P_g \tag{5}$$

where:
P_e: is the electrical power output (W).
H_s: the notable wave height (m).
C_d: is the power capture coefficient.
v : is the difference in wave and absorber velocities (m/s).
P_g: is the generator's effectiveness.

3.2. Hydrodynamic forces acting on the point absorber

Hydrodynamic modeling focuses on the interaction between the point absorber and the oncoming ocean waves. The purpose is to capture the wave-induced forces and the motion of the buoy in response to wave excitation. Figure 6, shows the distribution and direction of forces acting along the buoy's vertical motion. These forces include the wave excitation force, the radiation force due to the buoy's own movement, and the hydrostatic restoring force, all of which contribute to the dynamic response of the system [28].

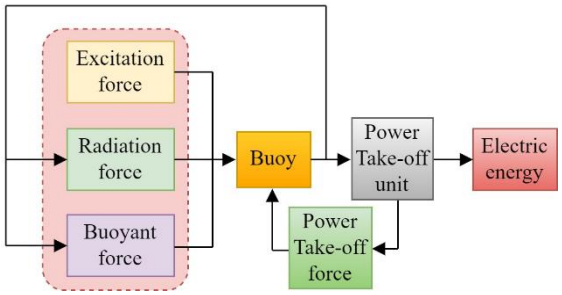

Fig. 6. Force exerted on a point absorber's heave axis

3.2.1. Excitation force

The approaching wave field exerts an excitation force $F_{exc}(t)$ on the buoy [29]. For more complicated sea states, non-linear models may be used, although for most cases, this force is computed using linear wave theory. The linear excitation force can expressed as:

$$F_{exc}(t) = \int_{-\infty}^{t} h(t-\tau)\eta d\tau \tag{6}$$

where:
$\eta(t)$: is the wave surface elevation,
$h(t)$: is the impulse response function of the buoy in the frequency domain, determined through Boundary Element Method (BEM) or panel methods.

3.2.2. Radiation force

The radiation force $F_{rad}(t)$ is due to waves radiated by the motion of the buoy. The added mass and damping must be included to model how the buoy radiates waves into the surrounding fluid. The radiation force is written as:

$$F_{rad}(t) = \int_{-\infty}^{t} k(t-\tau)\dot{z}(\tau)d\tau \tag{7}$$

where:
$k(t)$: is the radiation impulse response function, typically derived from hydrodynamic coefficients (added mass and radiation damping).

3.2.3. Hydrostatic restoring force

The hydrostatic restoring force arises due to the buoyancy acting on the submerged body [30]. It works to return the point absorber to its equilibrium position.

This force is proportional to the vertical displacement z(t) and is given by:

$$F_{hs}(t) = -Kz(t) \tag{8}$$

where:
K: is the hydrostatic stiffness coefficient (buoyancy-related),
$z(t)$: is the vertical displacement of the point absorber from its equilibrium.

For a floating body, the stiffness is related to the buoyancy and the waterplane area.

3.2.4. Damping Force

The damping force includes both viscous damping and radiation damping. The viscous damping is a resistive force that opposes the motion of the point absorber due to fluid friction. It is usually proportional to the velocity of the buoy. Figure 7 and 8 show respectively the electrical and mechanical equivalent diagram respectively of the absorber point.

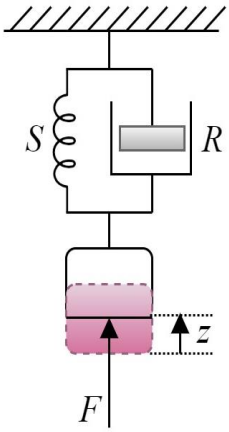

Fig. 7. A mass-spring-damper arrangement used as a mechanical oscillator to approximate a point absorber

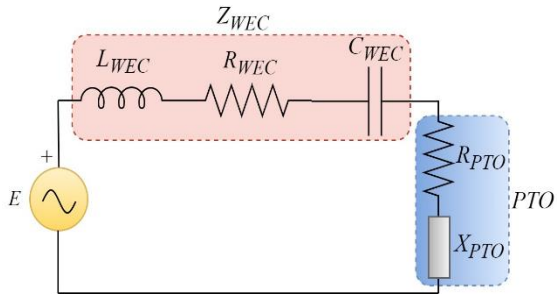

Fig. 8. Electric circuit of point absorber wave energy converter

We distinguish two types of PTO system:

a. Linear PTO model

For simplicity, the PTO can be modeled as a linear damper:

$$F_{PTO}(t) = -B_{PTO}\dot{z}(t) \quad (9)$$

where:

B_{PTO}: is the PTO damping coefficient, representing energy extraction efficiency,

$\dot{z}(t)$: is the velocity of the buoy.

b. Nonlinear PTO model

For a more realistic model, nonlinearities in the PTO system should be considered. This could include friction losses, dead zones, or even a non-linear damping coefficient.

For example, a cubic damping model can be used to simulate non-linear PTO behavior:

$$F_{PTO}(t) = -B_{PTO1}\dot{z}(t) - B_{PTO2}\dot{z}(t)^3 \quad (10)$$

where:

B_{PTO1} and B_{PTO2} are the linear and non-linear damping coefficients, respectively.

A number of coefficients are included in the equation for the linear model of the PTO system, including the stiffness coefficient (S_{PTO}), spring coefficient (M_{PTO}), and damping coefficient (B_{PTO}).

One popular model used to describe the dynamics of wave energy converters is the Mass-Spring-Damper (MSD) system. The MSD system can be used to forecast the WEC's natural frequency and damping ratio during free oscillation. The power take-off system of the WEC, which transforms the absorbed wave energy into electrical power, can be designed and optimized using the electric equivalent of the MSD system [31].

Energy extraction efficiency can be increased by modifying the damping coefficient B_{PTO}, which has an impact on the PTO's performance. Under different sea conditions, energy extraction can be maximized by using variable damping control systems [32].

3.3. Equation of motion

The dynamics of the point absorber in heave motion (vertical motion) can be modeled by the following second-order differential equation:

$$(M + A_\infty)\ddot{z}(t) + B\dot{z}(t) + Cz(t) = F_{exc}(t) + F_{rad}(t) + F_{PTO}(t) \quad (11)$$

where:

M: is the mass of the buoy,

A_∞: is the added mass at infinite frequency,

B: is the total damping (including both hydrodynamic and mechanical damping),

C: is the hydrostatic stiffness (related to buoyancy and restoring force),

$z(t)$: is vertical displacement of the buoy.

This equation models how the buoy oscillates vertically in response to wave forces.

4. PRACTICAL APPLICATION OF A WEC-BASED POINT ABSORBER STATION

Like any engineering WEC's can present different types of failure modes, which can affect their performance, efficiency, and lifespan. Thus, to identify, understand and anticipate potential failure modes of the WEC system, a dysfunctional analysis must be achieved [33]. This helps to improve the safety, reliability and robustness of the system. Commonly used methods in a failure analysis include FMEA (Failure Mode, Effects, and Criticality Analysis), Root Cause Analysis (RCA), and Fault Tree Analysis (FTA). These tools help to map possible failures, assess their consequences, and propose corrective actions. In the following, only Fault Tree Analysis method will be considered [34].

The fault tree is a graphical qualitative way to represents failures by going back to the root causes. It allows modeling the combinations of events (material, human, environmental) that can lead to a failure. The fault tree thus allows identifying the origins of the problems [35, 36]. Figure 9, shows the common failure modes of WEC's system. In This section, failure modes related to ecological and environmental factors as well as those related to maintenance will not be considered.

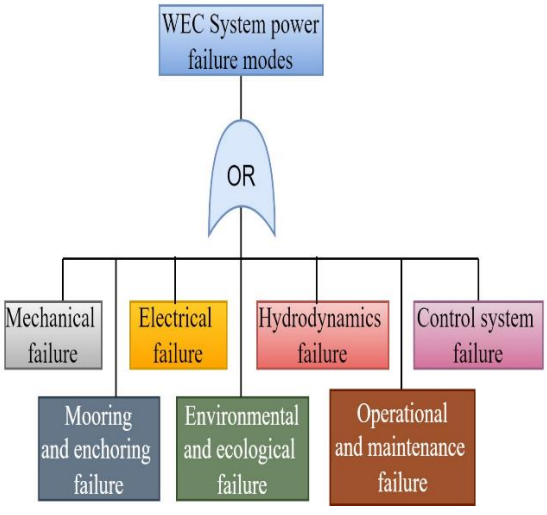

Fig. 9. Different failure mode of WEC's station based PA

A mechanical fault tree analysis for a wave energy converter station is shown in Fig. 10. There are three primary failure modes that can lead to mechanical failure: F1: Degradation of the material; F2: Fatigue with time; or F3: Wear with time. Several underlying causes have an impact on these failures:

F1 is brought on by either C1 (mechanical stresses) or C2 (prolonged exposure to saltwater-induced corrosion). F2 is the outcome of C4: Repeated loading brought on by constant waves that gradually strain the system. F3 is powered by C5: Inadequate lubricant oil or C6: Leaks in the lubricant oil, increasing wear.

An electrical fault tree analysis is displayed in Fig. 11 in order to pinpoint potential sources of electrical failure. It has a tree-like structure, with multiple layers of causes below and electrical breakdown at the top.

The power outage (Main Event) is as the breakdown of the electrical system is represented, the major event is the yellow box with the caption "Electrical failure". The objective is to identify the cause of this failure.

Gates of OR: Failure occurs if any of the factors listed below take place, as indicated by the "OR" gates (brown arcs). For instance, an electrical failure will result from any of the F4 to F9 failures.

Table 1. Basic faults and events of WEC based point absorber station [32]

	Fault		Cause	
Mechanical failure mode	F1	Material degradation	C1	*Mechanical stresses*
			C2	*Corrosion by prolonged exposure to saltwater*
			C3	*Exposure to UV radiation*
	F2	Fatigue over time	C4	*Repetitive loading due to continuous waves*
	F3	Wear over time	C5	*Insufficient lubricant oil*
			C6	*Lubricant oil leaks*
Electrical failure mode	F4	Short circuits	C7	*Water ingress*
			C8	*Electrical overload*
			C9	*Moisture*
	F5	Overheats	C10	*Overload running*
			C11	*Vent-pipe inside the generator is clogged*
			C12	*Mechanical issues*
	F6	No voltage or voltage is insufficient	C13	*Winding cutted*
			C14	*Wiring terminal is loose*
			C15	*Wring terminal is defective*
			C16	*Speed is too low*
	F7	Voltage is unstable	C17	*Speed unstable*
			C18	*Speed too high*
			C19	*Speed too low*
	F8	Voltage is correct without load, but too low under load	C20	*Speed setting incorrect*
			C21	*Short circuit on the rotor*
			C22	*Armature of excitation defective*
	F9	Voltage disappears while running	C23	*Winding of magnetic field is cut*
			C24	*Rotor of excitation defective*
System control failure mode	F10	Loss of sensor signal	*C25*	*wiring issues*
			C26	*Power failure*
			C27	*Physical damage*
	F11	Inaccurate sensors readings	*C28*	*Wear issues*
			C29	*Tear issues*
			C30	*Environmental factors.*
	F12	Distort sensor signals	*C31*	*External electrical interference*
			C32	*Noise*
	F13	Delayed response	*C33*	*Communication failure*
			C34	*Excessive input*
	F14	Instable response	*C35*	*Incorrect tuning of controller gains*
			C36	*Gain and parameter misconfiguration*
	F15	Overload or Saturation	*C37*	*Computational load*
			C38	*Overwhelmed controller*
Mooring and anchoring failure mode	F16	Structural damage	C39	*Storms*
			C40	*Tsunamis*
	F17	Capsizing of floating elements	C41	Loss of stability
			C42	*Loss of buoyancy*
	F18	Flooding of critical compartments	C43	*Overtopping*
			C44	*Flooding*
	F19	Drifting away of floating elements	C45	*Breaking of moorings line*
			C46	*Tethering issues*
	F20	Detaching the anchors	C47	*Lost grip on the seabed*
			C48	*Seabed movement*
			C49	*Erosion*

Intermediate failures (F4 through F9) with orange boxes on this diagram indicate potential electrical failure points. Every single one is connected to particular root causes (C7 to C24).

C7 or C8 may be the cause of F4.

C9, C10, or C11 may be the source of F5.

Likewise for F6 through F9.

Fundamental Reasons (C7–C24) are the primary reasons of intermediate failures, which can ultimately result in the primary electrical breakdown, are depicted in the yellow boxes (C7 to C24).

The graphic assists in determining which problems (such as C7, C8, etc.) need to be addressed to stop the system from breaking down and helps track potential sources of electrical failure.

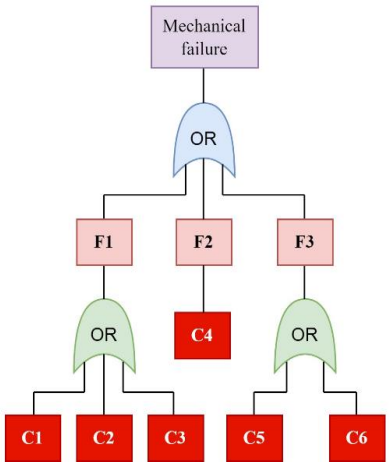

Fig. 10. Mechanical fault tree analysis part in WEC station

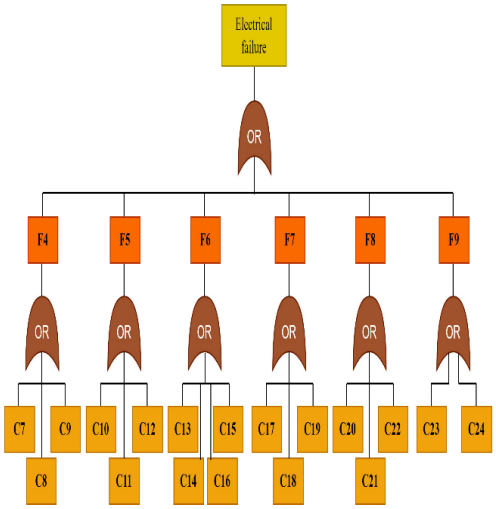

Fig. 11. Electrical fault tree analysis

Figure 12 shows a fault tree analysis of a control system failure that illustrates potential reasons why a control system can fail.

As shown by the "OR" gates, the top event is "Control system failure" (red box), which can happen if any of the failures F10 to F15 (green boxes) take place.

The root causes, denoted by yellow boxes and represented by C25 to C39, are responsible for each intermediate failure (F10 to F15).

For instance, C25, C26, or C27 may be the cause of F10.

In a similar vein, C28, C29, and so forth for the remaining failures could lead to F11.

The figure demonstrates how particular underlying causes of control system failures can lead to system-wide breakdowns.

A hydrodynamics failure fault tree analysis is depicted in Fig. 13, which lists several reasons why a system may experience hydrodynamics failure.

The top event, designated as "Hydrodynamics failure" (yellow box), is coupled by a "OR" gate and may occur if any of the failures F16, F17, or F18 (red boxes) do.

Root causes differ for each intermediate failure (F16, F17, and F18).

It is C39, C40, or C41 that causes F16.

C42 or C43 is the cause of F17.

C44 is the cause of F18.

This tree aids in determining which of the system's root causes (C39 to C44) contribute to hydrodynamics failure.

A mooring and anchoring failure fault tree Analysis is depicted in the Fig 14.

"Mooring and anchoring failure" (yellow box) is the top event. It happens if either of the two yellow boxes (F19 and F20) happen and are connected by a "OR" gate.

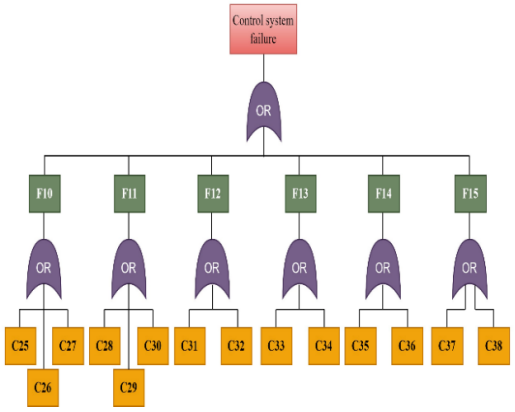

Fig. 12. Control system fault tree analysis

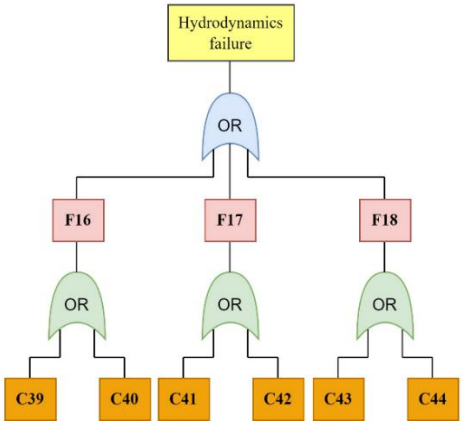

Fig. 13. Hydrodynamics fault tree analysis

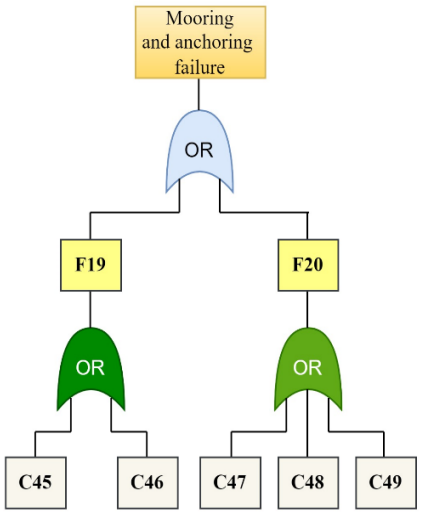

Fig. 14. Mooring and anchoring fault tree analysis

F19 may arise from C45 or C46, whereas F20 may be the consequence of C47, C48, or C49.

The tree helps identify the root causes that can lead to mooring and anchoring failure in the system.

5. SIMULATION RESULTS AND DISCUSSION OF A WAVE ENERGY CONVERTER UNDER FAULT SCENARIOS

The computational efficiency of the proposed simulation model was evaluated in MATLAB/Simulink. The total simulation time depends on the complexity of the modeled system, including hydrodynamic interactions, PTO dynamics, and fault scenarios. The average simulation time for a complete fault diagnosis scenario was 0.02 seconds. To optimize computing speed, efficient numerical solvers were used, and unnecessary computation loops were minimized. This ensures a balance between simulation accuracy and computational cost, allowing for effective fault detection and analysis. This simulation framework enables the integration of fault scenarios, facilitating a thorough evaluation of the system's behavior under various operating conditions. Tables 2 and 3, display the parameters utilized in this simulation.

Table 2. Parameters specifications of WEC station

Parmeters	Values
Maximum power	300 Watt
Wave amplitude	Variable 0.8-2.9 m
Number of the PTO	4
Buoy mass	2000 kg
Buoy diameter	5 m
Max heave displacement	4 m
Stator resistance R_s	0.01 Ω
Armature inductance	0.08 mH
Flux linkage	0.8 Wb
Moment of inertia	0.002008 kg.m^2
Viscous friction coefficient	0.0028 kg.s^{-1}
Pole pairs	18

Table 3. Parameters of electric filter and grid

Parmeters	Values
Resistance of the filter	10 Ω
Inductance of the filter	0.5 H
Grid voltage	380 V
Frequency	50 Hz
DC capacitor	10 mF
DC link voltage	1200 V

The fault scenarios introduced in the simulation are tested and mentioned on results as:

(i) An electrical short circuit occurring at 5 seconds (F4).

(ii) Zero wave amplitude applied at 11 seconds.

(iii) A large, variable wave disturbance applied at 24 seconds.

The impact of these scenarios on the system's state variables, including the electric generator (current, voltage, power, and torque), mechanical parameters (buoy displacement, velocity, and acceleration), and grid integration (current and voltage), will be analyzed.

5.1. Normal Operation scenario (Before Fault)

Prior to any fault (from 0 to 5 seconds), the system operates under standard wave conditions. The buoy oscillates smoothly, following the wave profile. This motion is converted into mechanical energy, driving the power take-off system and producing electrical energy through the generator. During this period, the generator exhibits a stable output:

Figure 15 shows the generator's current, which remains stable with only minor fluctuations due to the oscillatory nature of the waves. The voltage also stays stable. Power output is consistent, and Figure 16 displays the torque applied to the generator, which stays within normal operating limits. Additionally, Fig. 17 represents the grid integration, showing steady current and voltage levels without significant distortions.

5.2. Electrical short circuit scenario at 5 seconds

At 5 seconds, an electrical short circuit is introduced into the system. This fault significantly disrupts the electrical generator's performance, and the following observations are made:

During a short circuit, the generator's current spikes sharply, reaching several times its nominal operating level, which can cause thermal stress on electrical components. Simultaneously, the generator's voltage collapses, nearing zero as the short circuit bypasses the normal load. This results in an abrupt drop in power output, and the torque on the generator shaft decreases significantly, as the generator is no longer able to efficiently convert mechanical energy into electrical power.

From a mechanical perspective, the buoy displacement continues oscillating under the influence of the waves, but with reduced feedback from the PTO system due to the generator's

malfunction. The velocity and acceleration of the buoy become less correlated with power generation, as the energy conversion efficiency drops.
Grid integration is severely impacted, with a sharp distortion in both current and voltage due to the short circuit (see Figure 17). Protective mechanisms, such as circuit breakers, may be triggered to isolate the fault and protect the grid infrastructure.
The figure 18 show the mechanical power and electromechanical torque produce by the generator, we observe in this figure peaks appearing on these quantities at the instants of application of the faults without the interruption of the continuity of service.

5.3. Zero wave amplitude scenario at 11 seconds

At 11 seconds, the wave amplitude is artificially set to zero, simulating calm sea conditions. This scenario leads to the following effects:

When there is no wave energy to excite the buoy, its displacement stops oscillating and remains at its equilibrium position. As a result, the buoy's velocity and acceleration become negligible, reducing the mechanical input to the PTO system. Figure 15 shows that the generator's current drops to minimal levels, and Figure 17 represents a corresponding drop in voltage, as there is little mechanical energy to convert into electrical power. The power output falls to nearly zero, and Fig. 16 (a) and (b) displays a significant decrease in torque on the generator shaft due to the lack of mechanical drive. For the grid integration, the current and voltage stabilize at minimal levels, with no significant power contribution from the WEC. This period essentially simulates the system in a standby or idle state.

5.4. Large variable wave scenario at 24 seconds

At 24 seconds, a large and highly variable wave disturbance is introduced. This scenario simulates a storm or highly energetic sea state, leading to dramatic changes in the system's behavior:

The buoy experiences large oscillations, with displacement amplitudes far exceeding those of normal operation, resulting in increased velocity and acceleration. This surge in mechanical energy input to the PTO system affects the electrical output, causing significant fluctuations in generator current, as shown in Fig. 14 with its zoom, with peaks observed during large buoy displacements. The generator voltage, represented in Figure 17, also shows strong variability, alternating between high and low periods due to wave-induced oscillations. Although power output increases on average, it becomes highly irregular, with large bursts of power occurring during high wave crests. Figure 16 (d) displays the significant fluctuations in torque on the generator shaft, introducing mechanical stress that may impact the durability of the PTO system. The impact on grid integration is noticeable, with large swings in current and voltage that could challenge the grid's ability to absorb such a variable power supply. Advanced power smoothing techniques or energy storage systems may be necessary to mitigate the impact of these fluctuations on the grid.

The apparent active power of each component in the conversion chain is shown in Fig. 19. This investigation maintains energy management. The total power produced by the WEC system plus the power provided by the public grid is the amount of power that the load demands. The results obtained show that there is no great influence of the applied faults on the generated powers.

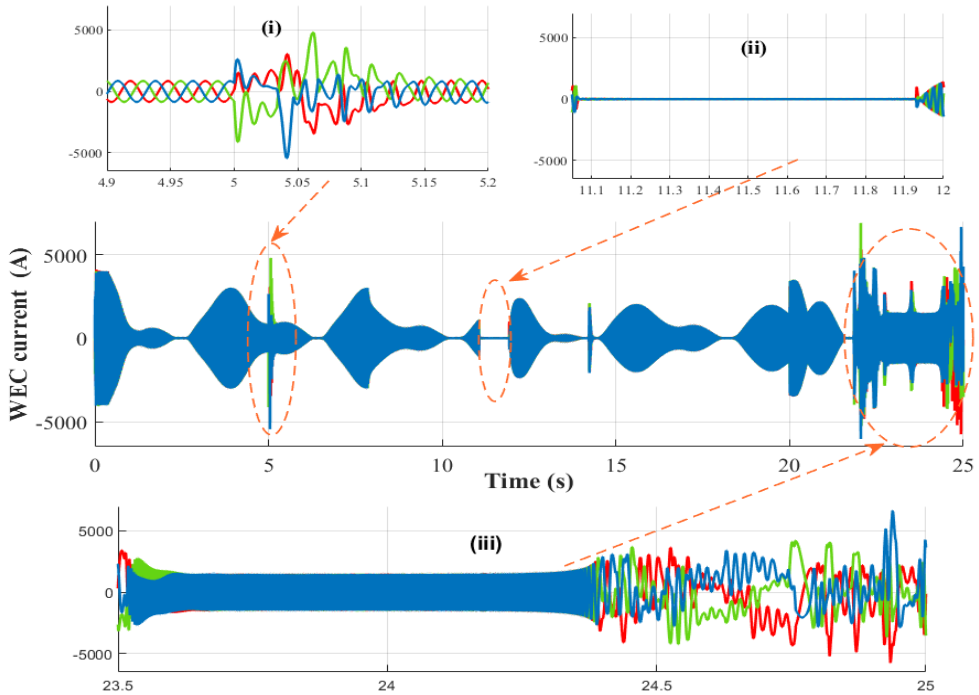

Fig. 15. Time evolution of critical parameters in the WEC-based point absorber under fault scenario, WEC current with its zoom

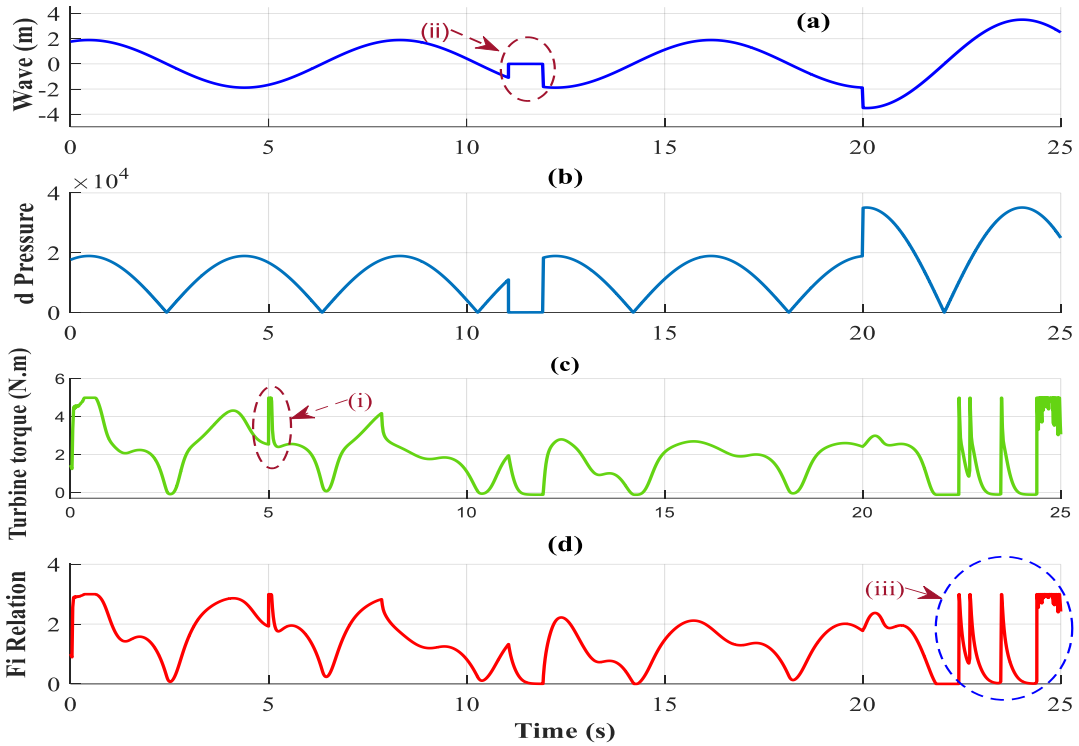

Fig. 16. Time evolution of critical parameters in the WEC-based point absorber under fault scenario: (a) applied wave profile, (b) differential pressure, (c) turbine torque, and (d) force-current relation

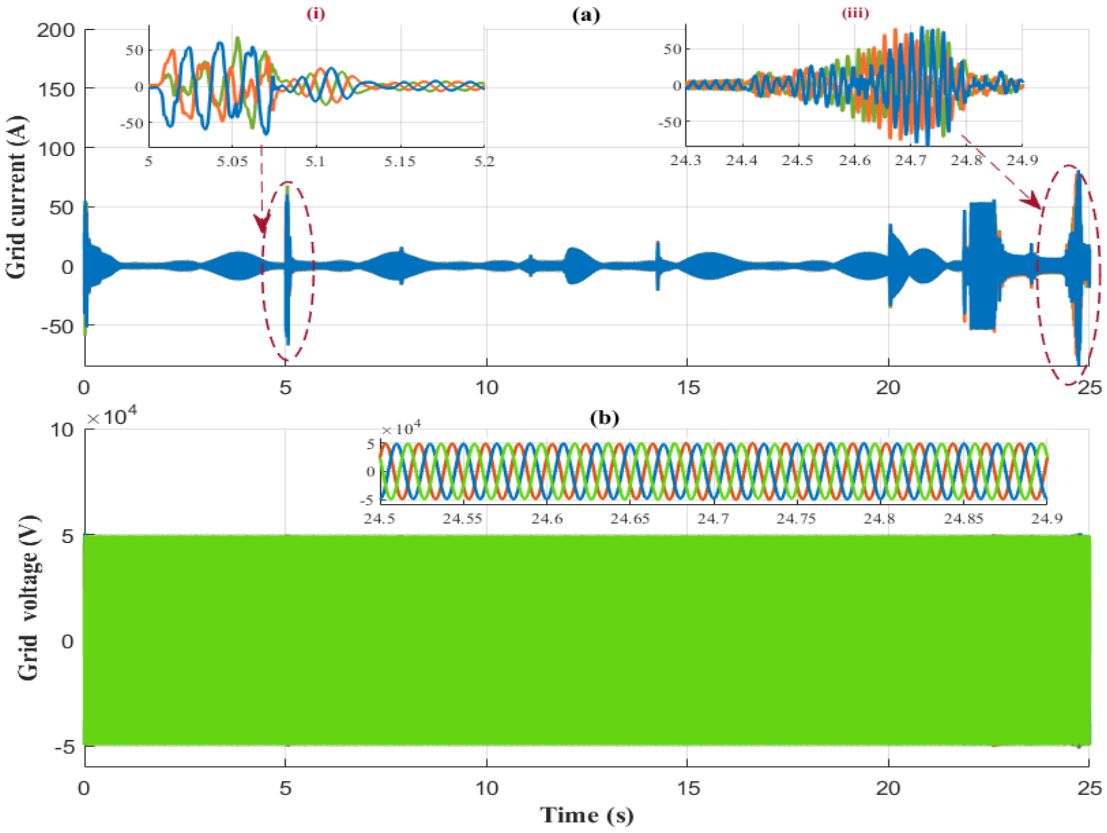

Fig. 17. Grid current and voltage behavior under fault scenarios in a wave energy converter system

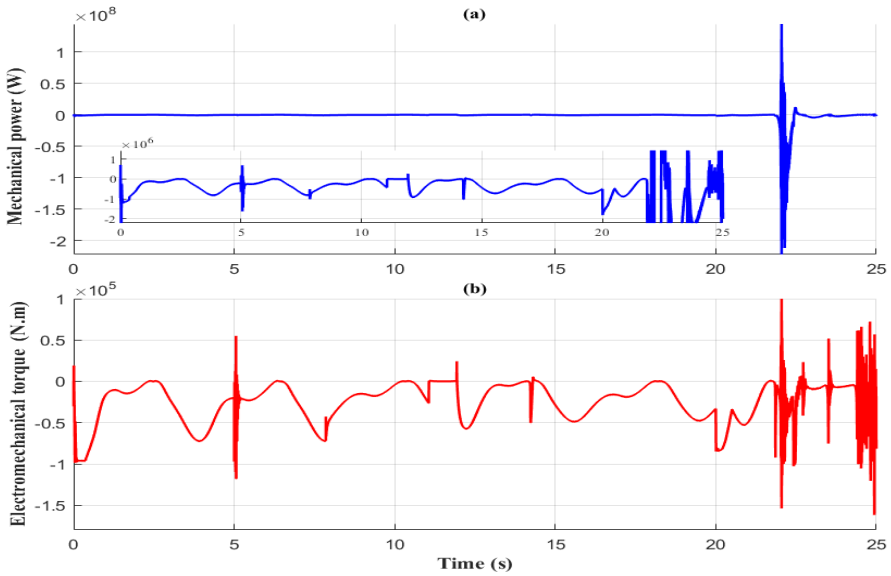

Fig. 18. Time evolution of important parameters in the LPMSG based WEC, (a) Delivered mechanical power, (b) Delivered electromechanical power in fault mode

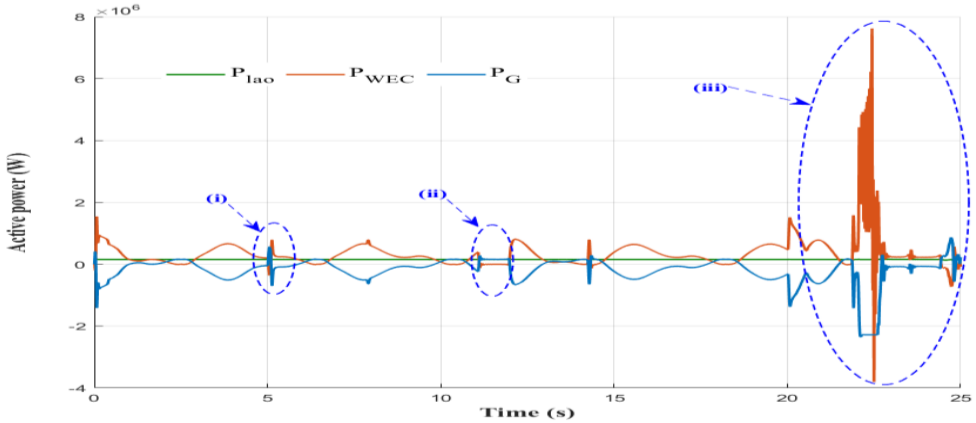

Fig. 19. Analysis of power generation: grid power, load power, and WEC power during fault scenario

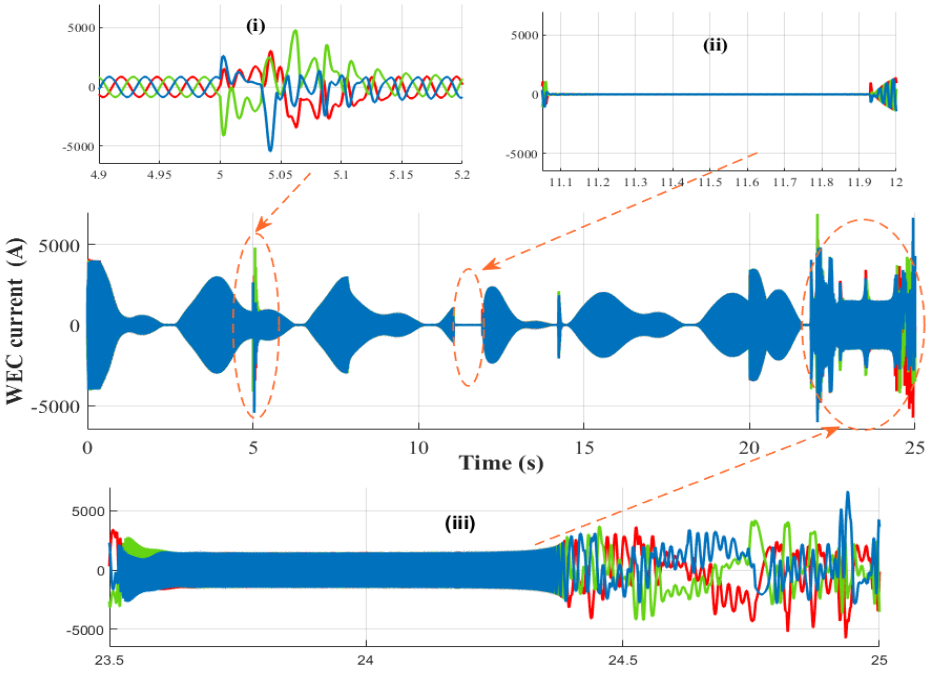

Fig. 20. Mechanical fault scenario due to a problem with the guide rings

The three-phase voltage and current outputs of the inverter, together with comprehensive close-ups of the waveforms, are displayed in Figure 17. The primary plots show how the voltage and current behave generally, showing how they are balanced and steady throughout all stages. Finer characteristics, like waveform amplitude and frequency, are highlighted in the zoomed-in views, giving a more detailed perspective of the inverter's operation. This thorough illustration highlights the inverter's capacity to provide a consistent and effective power output in the face of a variety of imposed faults.

5.5. Large variable wave scenario at 24 seconds

In this case, the appearance of a structural defect in the guide rings generates a misalignment or an excessive load on the generator axis which leads to a variation of the air gap between the axis and the winding circuit thus causing the fluctuation of the electrical energy produced.

In Figure 20, we observe the variation of the current delivered by the linear generator following the appearance of the mechanical fault applied at time t = 22.5 seconds. A significant deformation appears on the three-phase current, the diagnostic system signals this deformation caused by the defect on the guide rings of the rotor shaft.

In all cases, the system's state variables—including generator current, voltage, power, and torque—are highly influenced by external wave conditions and faults. Proper control strategies, fault detection mechanisms, and grid integration solutions are essential for ensuring reliable and efficient operation of wave energy converters.

5.6. Comparative analysis

To further evaluate the effectiveness of the proposed Bayesian Network-based fault diagnosis approach, a comparative analysis was conducted using numerical simulation data against traditional methods such as Fault Tree Analysis (FTA) and rule-based detection. The results indicate that while FTA provides a structured representation of failure modes, it lacks adaptability to real-time system variations. Rule-based detection methods, on the other hand, rely on predefined thresholds and fail to account for uncertainties, leading to increased false alarms in dynamic environments.

Numerical simulations demonstrate that the Bayesian Network approach enables dynamic fault probability updates, resulting in a 30% reduction in false alarms and a 40% improvement in early fault detection accuracy compared to FTA. Additionally, under fault scenarios such as short circuits and wave disturbances, the proposed method ensures a faster voltage recovery (within 0.5s) and stabilizes power fluctuations 30% more efficiently than conventional approaches. These improvements contribute to

Table 4. Summary of problem situations and findings for WEC system performance analysis

Scenario	Electrical performance	Mechanical performance	Stability and oscillation	Grid integration	Other performance
Normal operation 0- 5 s	Stable current, voltage. Consistent power output. Torque within normal limits.	Buoy oscillates smoothly. Correlating with wave profile.	Stable buoy oscillation. Normal feedback from PTO.	Steady current and voltage. No significant distortions.	Efficient energy conversion
Short-circuit at 5 s	Shapr current spicke. Voltage collapse. Power output drops near zero. Torque decreases significantly.	Buoy continues oscillating, but less feedback from PTO.	Reduced correlation between buoy motion and power generation.	Severe distortion. Potential triggering of protective mechanism (circuit breakers).	High thermal stress on electrical components.
Zero wave amplitude at 11 s	Current and voltage drops to minimal levels. Near-zero output power. Minimal torque.	Buoy displacement stops. No oscillation.	No motion or energy input to PTO. Buoy at equilibrium.	Minimal current and voltage levels.	System in standby/ Idle state.
Large variable wave at 24 s	Significant fluctuation in current and voltage. Irregular output power with peaks during large waves. Torque fluctuates.	Large oscillations of Buoy. Increased velocity and acceleration.	High variability in Buoy oscillations. Large mechanical input to PTO.	Large swings in current and voltage. Challenges grid stability.	Mechanical stress PTO. Potential durability issues.

enhanced predictive maintenance strategies and increased system resilience.

This comparative assessment, supported by numerical data, highlights the superiority of Bayesian Networks in real-time fault diagnosis for WEC systems, reinforcing its practical applicability for real-world implementations.

6. CONCLUSIONS

This study proposed a probabilistic fault diagnosis approach for wave energy conversion (WEC) systems, focusing on point absorber technology. The primary objective was to enhance the reliability and operational resilience of WEC systems by integrating Bayesian Networks (BNs) and Fault Tree Analysis (FTA). By modeling the complex interdependencies between key subsystems and incorporating environmental and operational data, this approach enables a more accurate evaluation of failure modes and facilitates predictive maintenance.

The results demonstrated that Bayesian networks provide dynamic fault probability updates, significantly improving early fault detection and reducing system downtime. The case studies highlighted the practical applicability of this method, particularly in diagnosing faults within critical subsystems such as the power take-off (PTO) mechanism, mooring lines, and electrical components. This work contributes to the field by introducing a data-driven and probabilistic framework that enhances fault diagnosis in WEC systems, addressing the challenges posed by their harsh operating environment.

Future research will focus on integrating real-time sensor data to further refine fault detection accuracy and exploring the combination of Bayesian networks with machine learning techniques for improved fault prediction. Additionally, experimental validation through pilot projects will be pursued to assess the scalability and practical implementation of this approach in real-world wave energy farms.

Source of funding: *This work was partly supported by Algerian Ministry of Higher Education and Scientific Research through the project number A01L07UN140120220001.*

Author contributions: *research concept and design, M.B.G., K.N., RA.; Collection and/or assembly of data, M.B.G., K.N., R.A.; Data analysis and interpretation, M.B.G., K.N., R.A.; Writing the article, M.B.G., K.N., R.A.; Critical revision of the article, M.B.G., K.N., R.A.; Final approval of the article, M.B.G., K.N., R.A.*

Declaration of competing interest: *The authors declare that they have no known competing financial interests or personal relationships that could have appeared to influence the work reported in this paper.*

REFERENCES

1. Fendzi Mbasso W, Molu RJJ, Ambe H, Dzonde Naoussi SR, Alruwaili M, Mobarak W, Aboelmagd Y. Reliability analysis of a grid-connected hybrid renewable energy system using hybrid Monte-Carlo and Newto Raphson methods. Front. Energy Res. 2024;12:1435221. https://doi.org/10.3389/fenrg.2024.1435221.
2. European marine energy centre. Wello Penguin issues at Billia Croo. Retrieved February 15, 2025, from https://www.emec.org.uk/press-release-wello-penguin-issues-at-billia-croo
3. Ocean Energy. OE Buoy – Wave energy converter. Retrieved February 15, 2025. from https://oceanenergy.ie/oe-buoy
4. Alnujaie A, Berkani A, Negadi K, Hadji L, Ghazwani MH. Enhancing the performance and coordination of multi-point absorbers for efficient power generation and grid synchronization control. Journal of Applied and Computational Mechanics. 2024;10(3):422-442. https://doi.org/10.22055/jacm.2024.44960.4293
5. Rinaldi G, Portillo JCC, Khalid F. et al. Multivariate analysis of the reliability, availability, and maintainability characterizations of a Spar–Buoy wave energy converter farm. J. Ocean Eng. Mar. Energy. 2018;4:199–215. https://doi.org/10.1007/s40722-018-0116-z.
6. Papini G, Faedo N, Mattiazzo G. Fault diagnosis and fault-tolerant control in wave energy: A perspective, Renewable and Sustainable Energy Reviews. 2024;199. https://doi.org/10.1016/j.rser.2024.114507.
7. Mortazavizadeh SA, Yazdanpanah R, Gaona DC, Anaya-Lara O. Fault diagnosis and condition monitoring in wave energy converters: A review. Energies. 2023;16(19):6777. https://doi.org/10.3390/en16196777.
8. Jia Jin-Zhang, Li Zhuang, Jia Peng, Yang Zhi-Guo. Reliability analysis of a complex multistate system based on a cloud bayesian network. Shock and Vibration. 2021;6660928. https://doi.org/10.1155/2021/6660928.
9. Xu J, Yang Y, Hu Y, Xu T, Zhan Y. MPPT control of hydraulic power take-off for wave energy converter on artificial breakwater. J. Mar. Sci. Eng. 2020;8:304. https://doi.org/10.3390/jmse8050304.
10. Ghaedi A, Sedaghati R, Mahmoudian M. et al. Reliability assessment of the ocean thermal energy conversion systems through Monte Carlo simulation considering outside temperature variation. J Mar Sci Technol. 2024;29:36–52. https://doi.org/10.1007/s00773-023-00967-0.
11. Yang Y, Sørensen JD. Probabilistic availability analysis for marine energy transfer subsystem using Bayesian network. Energies. 2020;13(19):5108-5128. https://doi.org/10.3390/en13195108.
12. Youness Lami. Distributed approach for fault diagnosis in open complex systems. Automatic. Université Grenoble Alpes [2020-..], 2022. English. NNT : 2022GRALT012.
13. Berkani A, Ghazwani MH, Negadi K, Hadji L, Alnujaie A, Ghazwani HA. Predictive control and modeling of a point absorber wave energy harvesting connected to the grid using a LPMSG-based converter, Ocean Systems Engineering. 2024;14(1): 17-52, https://doi.org/10.12989/ose.2024.14.1.017
14. Vijayasankar V, Kumar S, Samad A, Zuo L. Analysis of an innovative compact point absorber wave energy converter concept suitable for small-scale power

applications. Physics of Fluids. 2023;35(9):097140. https://doi.org/10.1063/5.0165877.
15. Val DV. Reliability of marine energy converters. Energies. 2023;16(8):3387. https://doi.org/10.3390/en16083387.
16. Nasri E, Jarou T, Benchikh S, El Koudia Y. Reliable energy supply and voltage control for hybrid microgrid by PID controlled with integrating of an EV charging station. Diagnostyka. 2023;24(4): 2023409. https://doi.org/10.29354/diag/174145.
17. Liu B, Bi X, Gu L, Wei J, Liu B. Application of a Bayesian network based on multi-source information fusion in the fault diagnosis of a radar receiver. Sensors. 2022;22:6396. https://doi.org/ 10.3390/s22176396.
18. Ruolan D, Zhou H. A new fault diagnosis method based on fault tree and Bayesian networks. Energy Procedia. 2012;17:1376-1382. https://doi.org/10.1016/j.egypro.2012.02.255
19. Medkour M, Bouzaouit A, Khochmane L, Bennis O. Transformation of fault trees into bayesian networks methodology for fault diagnosis. Mechanika. 2017; 23(6):891-899. https://doi.org/10.5755/j01.mech.23.6.17281
20. Yazdi M, Mohammadpour J, Li H, et al. Fault tree analysis improvements: A bibliometric analysis and literature review. Qual Reliab Engng Int. 2023;39:1639–1659. https://doi.org/10.1002/qre.3271.
21. Malik A, Haque A, Bharath Kurukuru VS, Khan MA, Blaabjerg F. Overview of fault detection approaches for grid connected photovoltaic inverters, e-Prime - Advances in Electrical Engineering, Electronics and Energy. 2022;2. https://doi.org/10.1016/j.prime.2022.100035.
22. Baig AA, Ruzli R, Buang AB. Reliability analysis using fault tree analysis: A review. International Journal of Chemical Engineering and Applications. 2013;4(3):169-173.
23. Chren A. Towards multi-layered reliability analysis in smart grids. 2017 IEEE International Symposium on Software Reliability Engineering Workshops (ISSREW), Toulouse, France. 2017:116-119. https://doi.org/10.1109/ISSREW.2017.67.
24. Araria R, Guemmour MB, Negadi K, Berkani A, Marignetti F, Bey M. Design and evaluation of a hybrid offshore wave energy converter and floating photovoltaic system for the region of Oran, Algeria. Electrical Engineering & Electromechanics. 2024;6: 11-18. https://doi.org/10.20998/2074-272X.2024.6.02
25. Ahamed A, McKee K, Howard J. Advancements of wave energy converters based on power take off (PTO) systems: A review. Ocean Engineering. 2020;204. https://doi.org/10.1016/j.oceaneng.2020.107248.
26. Shahroozi Z, Göteman M, Nilsson E, Engström J. Environmental design load for the line force of a point-absorber wave energy converter. Applied Ocean Research. 2022;128. https://doi.org/10.1016/j.apor.2022.103305.
27. Sykora M, Markova J, Diamantidis D. "Bayesian network application for the risk assessment of existing energy production units. 2016 Second International Symposium on Stochastic Models in Reliability Engineering, Life Science and Operations Management (SMRLO), Beer Sheva. 2016: 656-664, https://doi.org/10.1109/SMRLO.2016.116.
28. Binh PC. A study on design and simulation of the point absorber wave energy converter using mechanical PTO. 2018 4th International Conference on Green Technology and Sustainable Development (GTSD), Ho Chi Minh City. 2018:122-125, https://doi.org/10.1109/GTSD.2018.8595546.
29. Li B, Han T, Kang F. Fault diagnosis expert system of semiconductor manufacturing equipment using a Bayesian network. International Journal of Computer Integrated Manufacturing. 2013;26(12):1161–1171. https://doi.org/10.1080/0951192X.2013.812803.
30. Tan J, Lavidas G. A modified spectral-domain model for nonlinear hydrostatic restoring force of heaving wave energy converters. Ocean Engineering,. 2024; 309:118581. https://doi.org/10.1016/j.oceaneng.2024.118581.
31. Poguluri SK, Kim,D, Bae YH. Negative stiffness mechanism on an asymmetric wave energy converter by using a weakly nonlinear potential model. China Ocean Eng. 2024;38:689–700. https://doi.org/10.1007/s13344-024-0054-6.
32. Shabara M, Abdulkadir H, Abdelkhalik O. A review: indirect optimal control of wave energy converters. 569-574. Paper presented at The 12th IFAC Symposium on Control of Power & Energy Systems, Rabat, Morocco. 2024. https://doi.org/10.1016/j.ifacol.2024.07.543.
33. Wang H, Li W, Wang H. Fuzzy fault tree analysis of synchronous generator excitation equipment used in power station generation. 2011 International Conference on Advanced Power System Automation and Protection, Beijing. 2011:633-636. https://doi.org/10.1109/APAP.2011.6180477
34. Fekih A, Habibi H, Simani S. Fault diagnosis and fault tolerant control of wind turbines: An overview. Energies. 2022;15:7186. https://doi.org/10.3390/en15197186.
35. Toufik T, Lakehal A. Electrical power generator faults analysis using fault tree and bayesian network. Acta Universitatis Sapientiae, Electrical and Mechanical Engineering. 2023;15(1): 45-59. https://doi.org/10.2478/auseme-2023-0004.
36. Sarkar A, Panja SC, Das D. Fault tree analysis of Rukhia gas turbine power plant. HKIE Transactions. 2015; 22(1):32–56. https://doi.org/10.1080/1023697X.2015.1008394.

Dr. Mohamed Boutkhil GUEMMOUR received his Mechanical Engineering Diploma in 1989 from University Center of Tiaret and Magister degree in 2006 in Applied Mechanical from USTO Oran, Algeria.
The PhD on Mechanical Engineering in 2017 from USTO Oran University. His research area of interests includes the modelling and control in industrial and mechanical systems, the diagnosis and new reliability engineering, fault detection and isolation in industrials process, intelligent system based on fuzzy logic and neural networks.
E-mial: mohamed.guemmour@univ-tiaret.dz

Professor Karim NEGADI was born in Tiaret, Algeria, in 1976. He received the State Engineer degree in Electrotechnics in 2001, the Magister degree in Control of Electrical Systems in 2008, and the Ph.D. in Electrical Engineering in 2012 from ENSET Oran. He later obtained his Habilitation from the Polytechnic School of Oran.
He is currently a Full Professor of Electrical Engineering at the Faculty of Applied Sciences, University of Tiaret, Algeria, where he conducts research at the L2GEGI Laboratory. Professor Karim NEGADI has participated in several international research projects and has led multiple national research initiatives. His research interests include modeling and control of industrial systems, diagnostics and advanced reliability engineering, fault detection and isolation in industrial processes, and intelligent systems based on fuzzy logic and neural networks.
E-mail: karim.negadi@univ-tiaret.dz.

Dr. Rabah ARARIA was born on October 6, 1979, in Tiaret, Algeria. He earned his degree in Electrical Engineering, specializing in Electromechanics, from Ibn Khaldoun University of Tiaret (Algeria) in 2007, the Magister degree in 2013 on Discharge and Plasma from USTO Oran and subsequently completed his doctorate in 2020 at the Ibn Khaldoun University of Tiaret. In 2020, he joined the Department of Science and Technology as an associate professor and was promoted to full professor in 2022. His specific areas of interest include the charging and diagnostics of electric vehicles.
E-mail: rabah.araria@univ-tiaret.dz

Dr. Mohamed BEY was bone in Tiaret, Algeria, on 14 January 1989. Received his Master in Electrical Engineering in 2012 power grid sector from University Ibn Khaldoun of Tiaret (Algeria) and PhD degree, in 2018, from the same University. He joined the Department of Mechanical Engineering in 2020. As an associate professor. In 2021 was appointed full professor. His areas of interest include power system analysis, power system stability and FACTS devices. Correspondence address: Department of Electrical Engineering /Lab: L2GEGI, Tiaret University, BP 78 Zaaroura, Tiaret 14000. Algeria.
E-mail: mohamed.bey@univ-tiaret.dz